

- microscope using either a 60 \times water (NA 0.9) or 100 \times oil (NA 1.4) objective. An acquisition box of 100 pixels by 40 pixels was used to increase collection speed and zoomed to achieve pixel sizes between 0.2 and 0.4 μ m. Reduced speed Ca^{2+} imaging (0.06 to 1 Hz) used for RGD experiments (RGDS and RGEs from Sigma) and imaging of global growth cone transients was performed on the MRC 600 mounted on a Zeiss upright microscope using a 764 pixel by 512 pixel collection box and a 40 \times Fluor (NA 1.2) oil objective. For all experiments, laser power was attenuated to 1 to 10% of maximum using neutral density filters. Loose coverslips with adherent neurons were inverted for use with oil objectives by first sealing them on a coverslip with high-vacuum grease (Dow Corning). Inlet and outlet ports were left when necessary for exchange of solutions.
8. P. Lipp, E. Niggli, *Cell Calcium* **14**, 359 (1993).
 9. For combined Fluo-4/Fura-Red imaging, neurons loaded with 5 μ M Fluo-4-AM and 5 μ M Fura-Red-AM (in 0.01% pluronic acid) were excited with the 488-nm laser line of the MRC 1024 and images were collected at both 522 ± 35 and at ≥ 585 nm wavelengths. Fluorescence was quantified and changes were normalized to baseline using MetaMorph (Universal Imaging) or NIH Image (W. Rasband, NIH) software; events exceeding 10% of baseline fluorescence were scored as filopodial transients. Statistical significance was determined using Student's *t* test unless otherwise noted, and variance is reported \pm SEM.
 10. Web figures 1 and 2, Web table 1, and three Quick-time movies are available at Science Online at www.sciencemag.org/cgi/content/full/291/5510/1983/DC1.
 11. N. L. Allbritton, T. Meyer, L. Stryer, *Science* **258**, 1812 (1992).
 12. Cultures of dissociated spinal neurons and neural tube explants were prepared from stage 20 to 22 *Xenopus* embryos. Cells were grown at 20°C in MR containing 2 mM Ca^{2+} (3) on untreated tissue culture plastic or on various biological substrates coated onto tissue culture plastic or acid-washed glass coverslips, usually at saturating concentrations (LN, FN, VN, and Poly-D-lysine from Sigma; TN from Gibco).
 13. M. A. Schwartz, M. D. Schaller, M. H. Ginsberg, *Annu. Rev. Cell Dev. Biol.* **11**, 549 (1995).
 14. M. A. Bourdon, E. Ruoslahti, *J. Cell Biol.* **108**, 1149 (1989).
 15. R. O. Hynes, *Cell* **69**, 11 (1992).
 16. M. G. Cappelino et al., *Nature* **386**, 843 (1997).
 17. D. S. Sakaguchi, K. Radke, *Brain Res. Dev. Brain Res.* **97**, 235 (1996).
 18. P. C. Letourneau, T. A. Shattuck, *Development* **105**, 505 (1989).
 19. P. W. Grabham, D. J. Goldberg, *J. Neurosci.* **17**, 5455 (1997).
 20. D. Bray, K. Chapman, *J. Neurosci.* **5**, 3204 (1985).
 21. For analysis of filopodial lifetimes and for Ca^{2+} photorelease studies, neurons were labeled with green fluorescence protein-actin (GFP-actin) to enhance visualization of filopodia. Two individual blastomeres at the eight-cell stage were injected with 1 to 5 ng of capped GFP-actin mRNA (mMessage machine, Ambion). Filopodial lifetime measurements were made on growth cones from loaded (1 hour, 100 nM BAPTA AM; Molecular Probes), and unloaded cultures on 5, 10, or 50 μ g/ml TN. Motile growth cones were selected and imaged at 15-s intervals for 30 min with the MRC 600 using a 100 \times oil objective. Lifetimes were measured as described (20) using NIH Image software, except that filopodia present at the beginning of the observation period were included for analysis.
 22. M. Lu, W. Witke, D. J. Kwiatkowski, K. S. Kosik, *J. Cell Biol.* **138**, 1279 (1997).
 23. Combined β 1 integrin/phalloidin labeling was performed immediately after Fluo-4 imaging and rapid perfusion of cold fixative through the coverslip chamber. Mouse primary antiserum to β 1 integrin (1:50, AB 8C8; Developmental Studies Hybridoma Bank) was applied for 1 hour followed by 1:20 Oregon Green Phalloidin with secondary antibody (1:250, Alexa Fluor 568 goat antibody to mouse; Molecular Probes) for 1 hour. Immunofluorescent images of actin filaments and β 1

integrin receptors were captured using the MRC 1024. Integrin receptor clusters were defined on the basis of fluorescence intensity, and their areas were quantified using NIH Image software.

24. T. M. Gomez, F. K. Roche, P. C. Letourneau, *J. Neurobiol.* **29**, 18 (1996).
25. Substrate boundaries were created by protecting regions of culture dishes with Sylgard (Dow Corning) strips as described (26), except that boundaries were identified by including 5% tetramethyl rhodamine isothiocyanate (TRITC) (Molecular Probes) with the first substrate coated.
26. T. M. Gomez, P. C. Letourneau, *J. Neurosci.* **14**, 5959 (1994).
27. Average filopodial transient frequency was $2.7 \pm 0.7 \text{ min}^{-1}$ on TC and $1.3 \pm 0.3 \text{ min}^{-1}$ on LN. Data are from six filopodia of three growth cones on each substrate imaged at 1 Hz.
28. T. M. Gomez, N. C. Spitzer, *Nature* **397**, 350 (1999).
29. For Ca^{2+} photorelease experiments, GFP-actin expressing spinal cord explants were plated onto LN-coated glass coverslips. After 6 to 18 hours in culture, neurons were loaded with 2.5 μ M caged- Ca^{2+} (NP-EGTA AM; Molecular Probes) for 1 hour then rinsed in MR. Motile growth cones were positioned with their leading edge 10 μ m in front of a 20- μ m spot and imaged at 15-s intervals for approximately 30 min with the MRC 600 using a 100 \times oil objective. A programmable shutter (Uniblitz) pulsed this spot with 310- to 410-nm ultraviolet light filtered from a 100-W mercury lamp for a

duration of 200 ms every 10 s. The direction of neurite growth was measured from the center of the leading edge to middle of the neurite at the base of the growth cone using NIH Image. The maximum difference in the angle of neurite growth between 5 to 15 μ m of growth was scored. Neurites with a net extension of $< 5 \mu$ m over the 30-min period were not included. Photorelease of Ca^{2+} in selected filopodia was tested using non-GFP expressing neurons loaded with 2.5 μ M Fluo-4 and NP-EGTA.

30. G. C. Ellis-Davies, J. H. Kaplan, *Proc. Natl. Acad. Sci. U.S.A.* **91**, 187 (1994).
31. J. Q. Zheng, *Nature* **403**, 89 (2000).
32. K. Hong, M. Nishiyama, J. Henley, M. Tessier-Lavigne, M. Poo, *Nature* **403**, 93 (2000).
33. T. B. Kuhn, C. V. Williams, P. Dou, S. B. Kater, *J. Neurosci.* **18**, 184 (1998).
34. P. Fatt, B. Katz, *J. Physiol.* **117**, 109 (1952).
35. S. Koizumi et al., *Neuron* **22**, 125 (1999).
36. We thank I. Hsieh, A. Marnik, and J. Kaufman for technical assistance and K. Kalil and P. Letourneau for comments on the manuscript. We thank K. Yamada (National Cancer Institute) for providing antibodies that block the function of β 1 integrin, V. Lemmon (Case Western Reserve) for providing L1 and NCAD, and J. Hegmann (Basel) for providing the GFP-actin construct. Supported by a NIH NINDS fellowship to T.M.G. and by grants to N.C.S.

11 October 2000; accepted 31 January 2001

Requirement for the SLP-76 Adaptor GADS in T Cell Development

Jeff Yoder,¹ Christine Pham,^{2,3,4} Yoshie-Matsubayashi Iizuka,³ Osami Kanagawa,⁴ Stanley K. Liu,⁵ Jane McGlade,⁵ Alec M. Cheng^{2,3,4*}

GADS is an adaptor protein implicated in CD3 signaling because of its ability to link SLP-76 to LAT. A GADS-deficient mouse was generated by gene targeting, and the function of GADS in T cell development and activation was examined. GADS⁻ CD4⁻CD8⁻ thymocytes exhibited a severe block in proliferation but still differentiated into mature T cells. GADS⁻ thymocytes failed to respond to CD3 cross-linking in vivo and were impaired in positive and negative selection. Immunoprecipitation experiments revealed that the association between SLP-76 and LAT was uncoupled in GADS⁻ thymocytes. These observations indicate that GADS is a critical adaptor for CD3 signaling.

The development and function of T cells are regulated by signaling through the CD3 complex, which serves both the pre-T cell receptor (pre-TCR) and the TCR [(1) and references therein]. Cross-linking of CD3 induces protein tyrosine phosphorylation in a wide range of proteins. Among these phosphorylation targets are two adaptor proteins, LAT and SLP-76, which function in a coordinated fashion to activate a diverse set of signaling proteins (2–5). The critical function of SLP-

76 and LAT is supported by the observation that mice lacking SLP-76 or LAT exhibit an absolute block in early thymocyte development (6–8).

The function of SLP-76 is dependent on its association with LAT (9–13). This association is mediated by an adaptor known as GADS, which contains two SH3 domains flanking a SH2 domain and a linker region. GADS associates constitutively with SLP-76 through the binding of the GADS SH3 domain, and is recruited to LAT through binding of its SH2 domain to phosphotyrosine motifs on LAT upon TCR activation (9–11, 13). Besides GADS, Grb2 and possibly Grap are also implicated as adaptors for SLP-76 (4). Because mutant T cells or primary mast cells lacking LAT demonstrate reduced phosphorylation of SLP-76 upon receptor activa-

¹Medical Scientist Training Program; ²Center for Immunology; ³Division of Rheumatology, Department of Medicine; ⁴Department of Pathology and Immunology; Washington University School of Medicine, St. Louis, MO 63110, USA. ⁵Hospital for the Sick Children, University of Toronto, Toronto, Canada.

*To whom correspondence should be addressed. E-mail: acheng@im.wustl.edu

tion (14–16), the association of SLP-76 with LAT may also couple to the induction of SLP-76 phosphorylation.

To address the function of GADS in vivo, GADS-deficient mice were generated by a gene-targeting approach (Fig. 1A) (17). In contrast to SLP-76⁻ mice, which frequently succumb to severe systemic hemorrhage at an early perinatal stage (7, 18), GADS⁻ mice were grossly healthy.

GADS⁻ mice had approximately fourfold fewer thymocytes than did wild-type littermates (Fig. 1C). Fluorescence-activated cell sorting (FACS) analysis for CD4, CD8, and TCR-β chain expression revealed that GADS⁻ thymocytes exhibited several developmental defects (Fig. 1, D and E). GADS⁻

mice had a modest increase in the percentage of CD4⁻CD8⁻ double negative (DN) thymocytes and a decrease in the percentages of CD4 and CD8 single positive (SP) thymocytes (Fig. 1D). TCR-β chain staining revealed a reduction in mature cells expressing high levels of TCR (Fig. 1E). In the peripheral T cell pool, CD4 T cells were most affected, with a reduction of up to 10-fold, whereas CD8 T cells were reduced by about twofold (Fig. 1F). However, the total number of peripheral CD4 cells did accumulate over time, indicating that GADS is not critical for the survival of mature T cells. In contrast to its effect on T cell development, GADS deficiency did not influence the development of B cells or other cell lineages (17).

To characterize the developmental defect in the DN thymocytes of GADS⁻ mice, we dissected the DN compartment using FACS analysis of CD44 and CD25 expression (19). As shown in +/+ mice, approximately 26% of the DN cells had progressed into the CD44⁻CD25⁻ (pro-T4 stage) (Fig. 2A). In contrast, GADS⁻ thymocytes exhibited a severe developmental arrest at the CD44⁻CD25⁺ (pro-T3) stage, the point at which pre-TCR signaling is first required (20, 21). Unlike RAG-2⁻ thymocytes, which are arrested in the DN stage, GADS⁻ thymocytes were able to differentiate into DP cells (Fig. 1C). This result suggests that GADS deficiency does not severely compromise the differentiation capacity of the pre-TCR.

The severe reduction of pro-T4 cells in GADS⁻ mice may have resulted from a specific defect in proliferation induced by the pre-TCR. To test this hypothesis, thymocytes gated on the pro-T3 subset were analyzed for cell size distribution. In contrast to wild-type cells, the GADS⁻ pro-T3 population contained significantly fewer large cells (Fig. 2B), previously characterized as actively dividing precursors of pro-T4 cells (21). The defect in proliferation of the pro-T3 population in GADS⁻ mice was confirmed by comparing the DNA content of CD25⁺ DN thymocytes (Fig. 2C).

Cross-linking of CD3 in RAG-2⁻ mice induces the differentiation and expansion of DN cells into DP cells, presumably by activating the pre-TCR signaling pathway (22). To examine whether GADS⁻ thymocytes had defects in CD3 signaling, we compared the effects of CD3 cross-linking in vivo in wild-type, RAG-2⁻, and GADS⁻ mice. Wild-type mice injected with antibody to CD3 exhibited accelerated development of DN thymocytes, as shown by a significant increase in pro-T4 cells (Fig. 2D). Cross-linking of CD3 also significantly promoted the development of RAG-2⁻ thymocytes, resulting in an expanded population of DP thymocytes (200 × 10⁶ cells, *n* = 3). By contrast, GADS⁻ mice treated with the antibody to CD3 exhibited no significant change in the developmental profile and none showed a significant increase in thymocyte numbers. Consistent with this observation, CD44/CD25 staining and cell size analysis revealed the lack of cellular expansion in the pro-T3 and pro-T4 compartments (Fig. 2D).

Cross-linking of CD3 in wild-type mice also induces cell death predominantly in the DP population, an effect thought to mimic thymic negative selection (Fig. 2E) (23). However, in vivo cross-linking of CD3 in GADS⁻ mice did not induce a significant deletion of the DP thymocytes (Fig. 2E) and had no effect on the total number of thymocytes. These results indicate that GADS is an integral part of CD3 signaling. Consistent

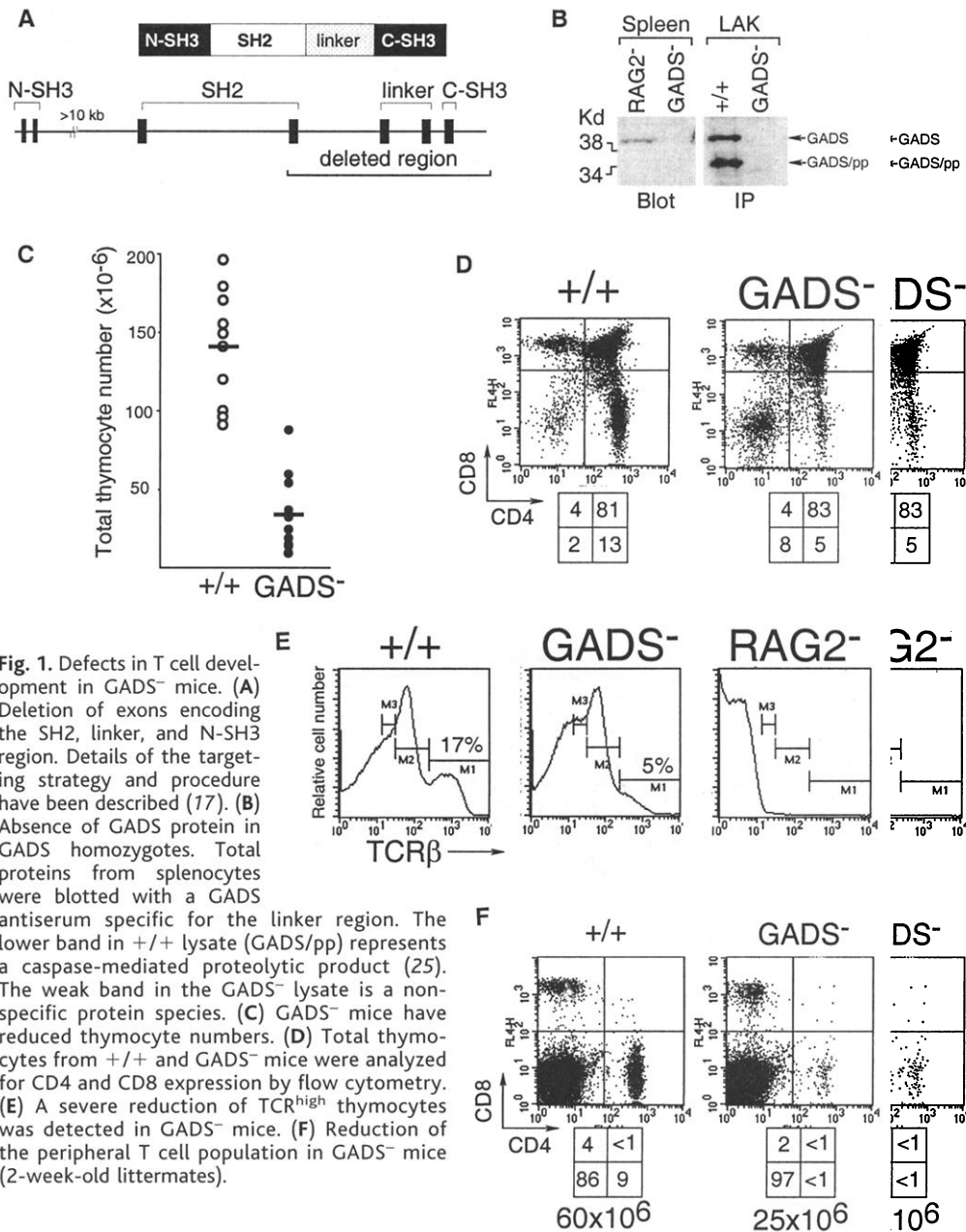


Fig. 1. Defects in T cell development in GADS⁻ mice. (A) Deletion of exons encoding the SH2, linker, and N-SH3 region. Details of the targeting strategy and procedure have been described (17). (B) Absence of GADS protein in GADS homozygotes. Total proteins from splenocytes were blotted with a GADS antiserum specific for the linker region. The lower band in +/+ lysate (GADS/pp) represents a caspase-mediated proteolytic product (25). The weak band in the GADS⁻ lysate is a non-specific protein species. (C) GADS⁻ mice have reduced thymocyte numbers. (D) Total thymocytes from +/+ and GADS⁻ mice were analyzed for CD4 and CD8 expression by flow cytometry. (E) A severe reduction of TCR^{high} thymocytes was detected in GADS⁻ mice. (F) Reduction of the peripheral T cell population in GADS⁻ mice (2-week-old littermates).

REPORTS

with this conclusion, CD69 up-regulation was compromised in GADS⁻ thymocytes (17).

To test the function of GADS in thymic selection, GADS⁻ mice were crossed with

mice carrying an $\alpha\beta$ TCR transgene specific for the male H-Y antigen (24). In $+/+$ male HY mice, clonotypic T cells undergo extensive negative selection, resulting in the severe depletion of DP cells and greatly diminished

thymocyte numbers. In contrast, GADS⁻ HY⁺ thymocytes did not exhibit negative selection in male mice, as shown by the persistent DP population (Fig. 3A). The ability of GADS⁻ thymocytes to undergo positive

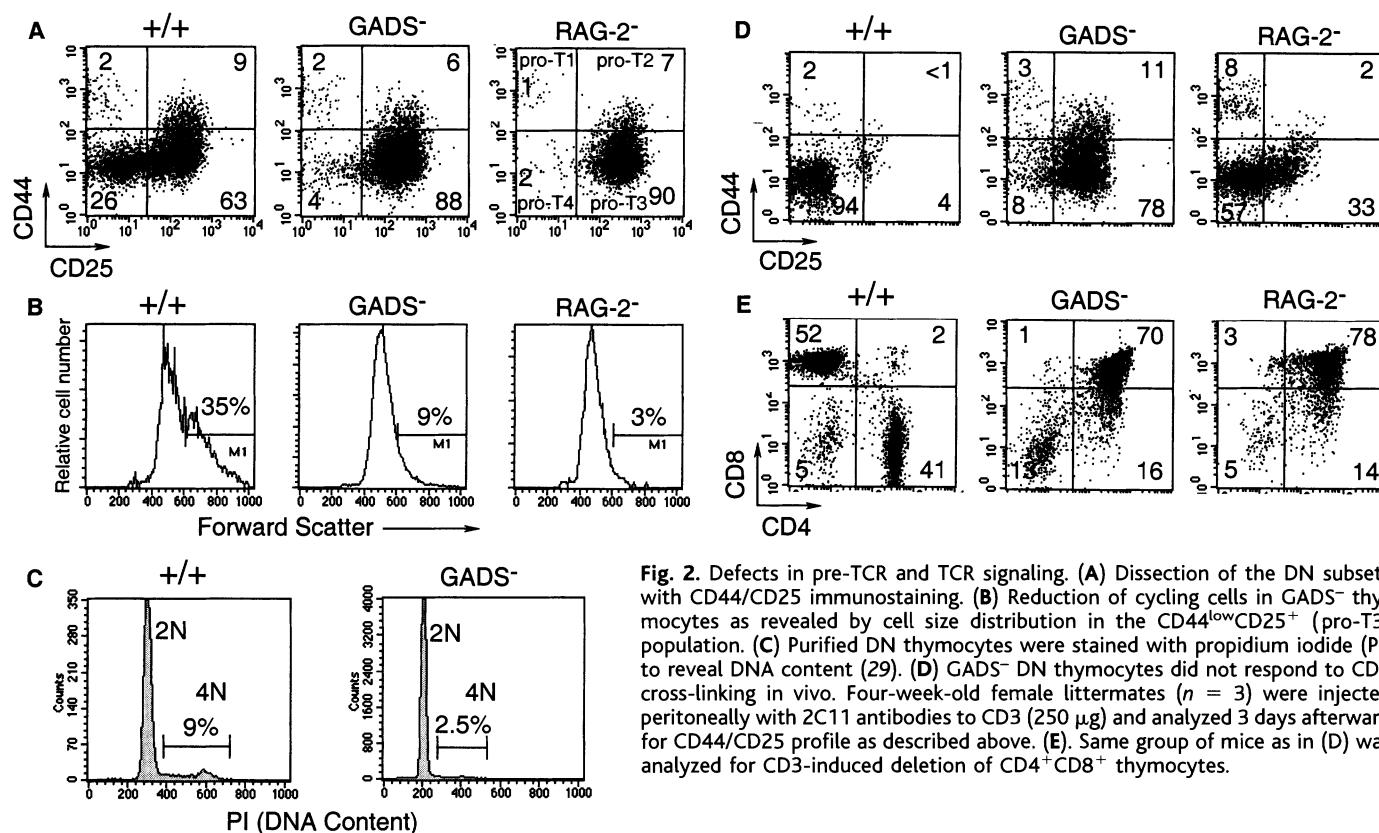


Fig. 2. Defects in pre-TCR and TCR signaling. (A) Dissection of the DN subsets with CD44/CD25 immunostaining. (B) Reduction of cycling cells in GADS⁻ thymocytes as revealed by cell size distribution in the CD44^{low}CD25⁺ (pro-T3) population. (C) Purified DN thymocytes were stained with propidium iodide (PI) to reveal DNA content (29). (D) GADS⁻ DN thymocytes did not respond to CD3 cross-linking in vivo. Four-week-old female littermates ($n = 3$) were injected peritoneally with 2C11 antibodies to CD3 (250 μ g) and analyzed 3 days afterward for CD44/CD25 profile as described above. (E) Same group of mice as in (D) was analyzed for CD3-induced deletion of CD4⁺CD8⁺ thymocytes.

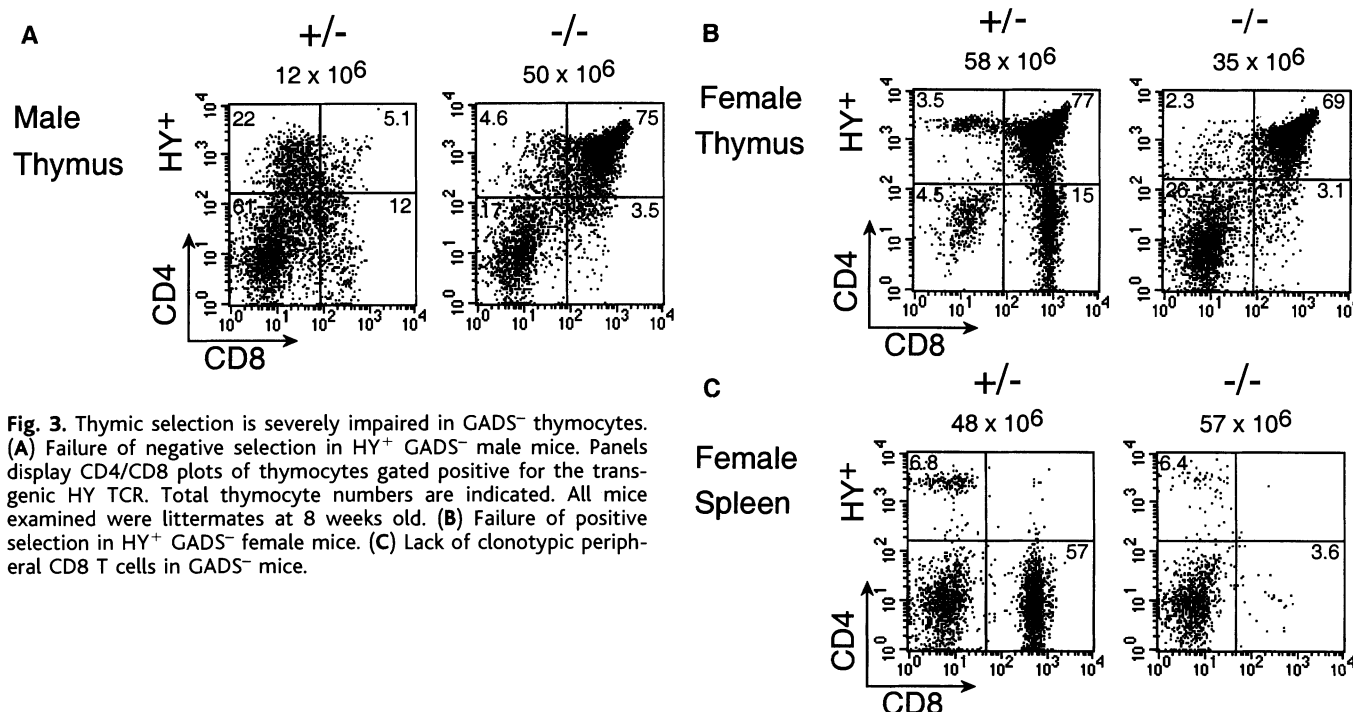


Fig. 3. Thymic selection is severely impaired in GADS⁻ thymocytes. (A) Failure of negative selection in HY⁺ GADS⁻ male mice. Panels display CD4/CD8 plots of thymocytes gated positive for the transgenic HY TCR. Total thymocyte numbers are indicated. All mice examined were littermates at 8 weeks old. (B) Failure of positive selection in HY⁺ GADS⁻ female mice. (C) Lack of clonotypic peripheral CD8 T cells in GADS⁻ mice.

selection in HY transgenic female mice, which lack the H-Y antigen, was also examined (Fig. 3B). In contrast to the wild-type HY⁺ thymocytes, which underwent positive selection to become predominantly CD8 T cells, GADS⁻ HY⁺ thymocytes failed to develop into mature CD8 cells (Fig. 3B). Similar defects in the positive selection of CD4 T cells were observed in transgenic mice expressing the DO11.10 TCR (25).

To investigate whether these defects in thymocyte development and activation are consistent with the adaptor function of GADS, we examined whether SLP-76 phosphorylation or association with LAT was compromised in GADS⁻ thymocytes. Cell lysates from total thymocytes activated by CD3 cross-linking were immunoprecipitated for SLP-76 and immunoblotted with an antibody to phosphotyrosine. Upon CD3 cross-linking, GADS⁻ thymocytes exhibited a significant increase in SLP-76 phosphorylation, which indicates that GADS is not required to mediate SLP-76 phosphorylation (Fig. 4A). Despite this observation, the association of SLP-76 with a phosphoprotein of approximately

40 kD was specifically reduced. Based on the molecular size and the pattern of induced phosphorylation, this 40-kD species is most likely to be LAT. Unfortunately, a direct demonstration of the LAT identity is restricted by the sensitivity of immunoblotting assay required for the detection of LAT in the trimolecular SLP-76/GADS/LAT complex. Based on the interaction between Grb2 and SLP-76 in vitro (4), it is possible that Grb2 may substitute for GADS in the GADS-deficient cells. We investigated this possibility by immunoprecipitating Grb2 from total thymocytes and immunoblotting for SLP-76 or SoS, but found no evidence of increased Grb2 association with SLP-76 (17).

Biochemical studies suggest that ITK bound to SLP-76 is recruited to LAT in order to phosphorylate and activate PLC-γ1 (3, 26). In accordance with this model, GADS⁻ thymocytes exhibited significantly reduced PLC-γ1 phosphorylation (Fig. 4B), and GADS-deficient T cells failed to flux calcium upon CD3 activation (Fig. 4C). GADS⁻ T cells activated with antigen proliferated to an extent comparable to that of the wild type

(25), a result that may be due to compensation during thymic development. Inducible gene targeting of GADS is required to further address this possibility. Although GADS is also expressed in the B cell lineage (11), our analysis indicated that GADS is not required for B cell activation (17).

This study provides genetic evidence that GADS is important for pre-TCR and TCR signaling. Mice deficient in GADS exhibit less severe defects, such as the lack of hemorrhage and the presence of DP and SP thymocytes, than do mice deficient in SLP-76. Such a phenotypic difference indicates that not all functions of SLP-76 are mediated through GADS. Despite the importance of GADS in the various aspects of thymocyte development, there is only a four- to sixfold reduction in total thymocyte number. This moderate reduction in thymocyte number may be due to the lack of efficient positive selection, which impairs the maturation of DP thymocytes; combined with the lack of negative selection, which limits the deletion of self-reactive thymocytes. GADS deficiency has a more pronounced effect in the maturation of the CD4 than the CD8 lineage. It has been proposed that the Ras pathway may quantitatively regulate the development of the CD4 and CD8 lineages (27). In this context, it is important to note that Ras activation by the SLP-76/LAT complex is regulated by at least two different pathways: one via Grb2-SoS bound to LAT and the other via RasGRP (28), which is activated by diacylglycerol and in principle lies downstream of PLC-γ1, whose activation is dependent on GADS-SLP-76. It will be interesting to address the differential effects in the maturation of CD4 and CD8 cells caused by these two pathways. Finally, the observation that LAT (14, 15), but not GADS, is required for the optimal phosphorylation of SLP-76 suggests that LAT has a yet-undefined role in SLP-76 phosphorylation. Further studies on the mechanism of SLP-76 phosphorylation may provide insight into this issue.

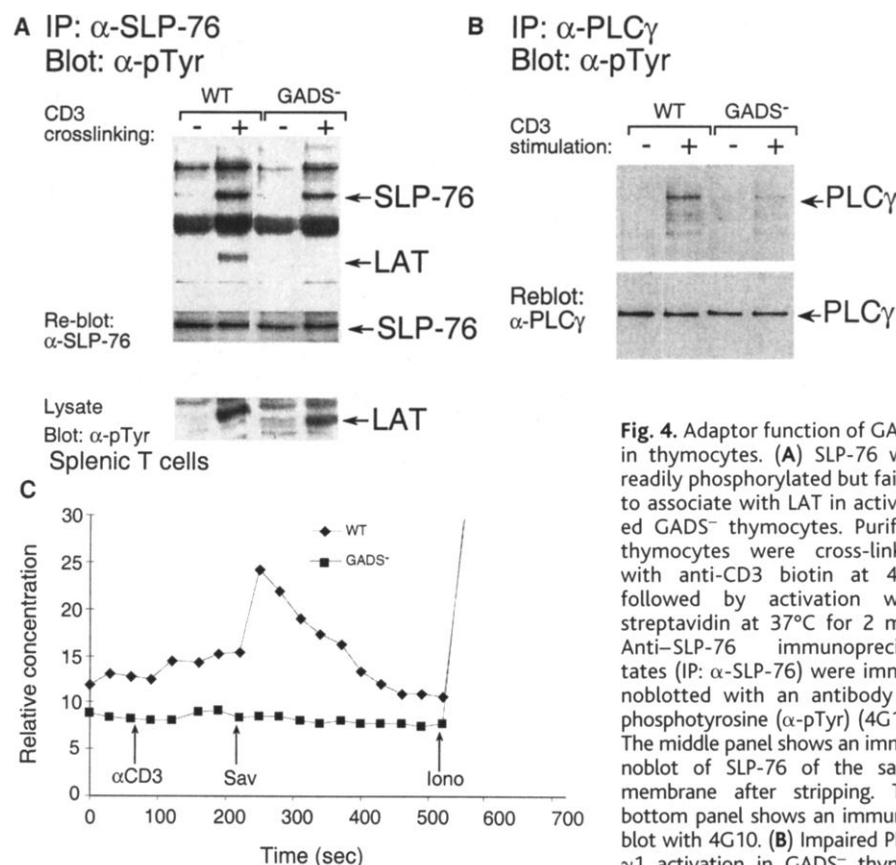


Fig. 4. Adaptor function of GADS in thymocytes. (A) SLP-76 was readily phosphorylated but failed to associate with LAT in activated GADS⁻ thymocytes. Purified thymocytes were cross-linked with anti-CD3 biotin at 4°C, followed by activation with streptavidin at 37°C for 2 min. Anti-SLP-76 immunoprecipitates (IP: α-SLP-76) were immunoblotted with an antibody to phosphotyrosine (α-pTyr) (4G10). The middle panel shows an immunoblot of SLP-76 of the same membrane after stripping. The bottom panel shows an immunoblot of PLC-γ1 with 4G10. (B) Impaired PLC-γ1 activation in GADS⁻ thymocytes. Lysates from activated thymocytes were immunoprecipitated for PLC-γ1 (IP: α-PLC-γ1) and immunoblotted with the 4G10 antibody to phosphotyrosine. The bottom panel shows an immunoblot of PLC-γ1 of the same membrane after stripping. (C) Defective calcium mobilization in GADS⁻ peripheral T cells. Total splenic T cells were stained with an APC-conjugated CD8 antibody and loaded with Fluo-4 to determine calcium flux in a FACS Calibre. Samples were first incubated with a biotinylated antibody to CD3 (αCD3) at 4°C, followed by cross-linking with streptavidin (Sav) at 37°C. Ionomycin (Iono) was added at the end of the experiment as a positive control.

References and Notes

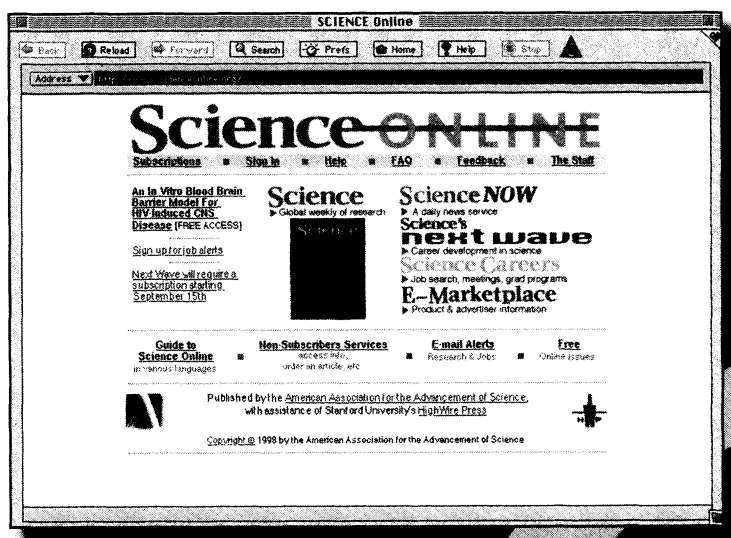
1. A. C. Chan, A. S. Shaw, *Curr. Opin. Immunol.* **8**, 394 (1996).
2. J. Bubeck-Wardenburg et al., *Immunity* **9**, 607 (1998).
3. S. C. Bunnell et al., *J. Biol. Chem.* **275**, 2219 (2000).
4. J. K. Jackman et al., *J. Biol. Chem.* **270**, 7029 (1995).
5. W. Zhang, J. Sloan-Lancaster, J. Kitchen, R. P. Tribble, L. E. Samelson, *Cell* **92**, 83 (1998).
6. J. L. Clements et al., *Science* **281**, 416 (1998).
7. V. Pivniouk et al., *Cell* **94**, 229 (1998).
8. W. Zhang et al., *Immunity* **10**, 323 (1999).
9. H. Asada et al., *J. Exp. Med.* **189**, 1383 (1999).
10. R. P. Bourette et al., *EMBO J.* **17**, 7273 (1998).
11. C. L. Law et al., *J. Exp. Med.* **189**, 1243 (1999).
12. S. K. Liu, C. J. McGlade, *Oncogene* **17**, 3073 (1998).
13. S. K. Liu, N. Fang, G. A. Koretzky, C. J. McGlade, *Curr. Biol.* **9**, 67 (1999).
14. W. Zhang, B. J. Irvin, R. P. Tribble, R. T. Abraham, L. E. Samelson, *Int. Immunol.* **11**, 943 (1999).
15. T. S. Finco, T. Kadlecck, W. Zhang, L. E. Samelson, A. Weiss, *Immunity* **9**, 617 (1998).
16. S. Saitoh et al., *Immunity* **12**, 525 (2000).

REPORTS


17. Supplementary information is available at www.sciencemag.org/cgi/content/full/291/5510/1987/DC1.
18. J. L. Clements *et al.*, *J. Clin. Invest.* **103**, 19 (1999).
19. H. R. Rodewald, H. J. Fehling, *Adv. Immunol.* **69**, 1 (1998).
20. H. J. Fehling, A. Krotkova, C. Saint-Ruf, H. von Boehmer, *Nature* **375**, 795 (1995).
21. E. S. Hoffman *et al.*, *Genes Dev.* **10**, 948 (1996).
22. Y. Shinkai, F. W. Alt, *Int. Immunol.* **6**, 995 (1994).
23. C. N. Levelt, A. Ehrfeld, K. Eichmann, *J. Exp. Med.* **177**, 707 (1993).
24. P. Kisielow, H. Bluthmann, U. D. Staerz, M. Steinmetz, H. von Boehmer, *Nature* **333**, 742 (1988).
25. Unpublished results.
26. E. M. Schaeffer *et al.*, *Science* **284**, 638 (1999).
27. L. L. Sharp, D. A. Schwarz, C. M. Bott, C. J. Marshall, S. M. Hedrick, *Immunity* **7**, 609 (1997).
28. J. O. Ebinu *et al.*, *Science* **280**, 1082 (1998).
29. Thymic DN cells were purified by Dynal magnetic beads. Purified samples were stained with antibody to CD25-FITC, washed, and fixed in 70% ethanol. Cells were washed and treated with propidium iodide (10 mg/ml) and ribonuclease A (250 mg/ml). Cells were gated for singlets and CD25⁺, and DNA content was determined by FL2-H.
30. We thank A. C. Chan and laboratory for many suggestions, technical advice, and generous gifts of reagents, and the Dr. Hector Molina laboratory for help and support. Supported by a research startup fund provided by the Department of Medicine and the Department of Pathology and Immunology at the Washington University School of Medicine.


6 November 2000; accepted 26 January 2001


Enhance your AAAS membership with the Science Online advantage.





Science ONLINE


 **Full text Science**—research papers and news articles with hyperlinks from citations to related abstracts in other journals before you receive *Science* in the mail.

 **ScienceNOW**—succinct, daily briefings, of the hottest scientific, medical, and technological news.

 **Science's Next Wave**—career advice, topical forums, discussion groups, and expanded news written by today's brightest young scientists across the world.

 **Research Alerts**—sends you an e-mail alert every time a *Science* research report comes out in the discipline, or by a specific author, citation, or keyword of your choice.

 **Science's Professional Network**—lists hundreds of job openings and funding sources worldwide that are quickly and easily searchable by discipline, position, organization, and region.

 **Electronic Marketplace**—provides new product information from the world's leading science manufacturers and suppliers, all at a click of your mouse.

All the information you need...in one convenient location.

Visit Science Online at <http://www.scienceonline.org>, call 202-326-6417, or e-mail membership2@aaaas.org for more information.

AAAS is also proud to announce site-wide institutional subscriptions to Science Online. Contact your subscription agent or AAAS for details.

